AECL EACL

AECL CANDU EACL CANDU

Influence of Graphite Discs, Chamfers, and Plenums on Temperature Distributions in High Burnup Fuel

AECL-9944

1990 April Avril 1990

AECL EACL

AECL CANDU EACL CANDU

Influence of Graphite Discs, Chamfers, and Plenums on Temperature Distributions in High Burnup Fuel

AECL-9944

by A. Ranger*, M. Tayal*, P. Singh*,
I.A. El-Osery **, and K.A. Yasso**

Presented at:
The 3rd International Conference on Simulation Methods in Nuclear Engineering

Montreal, Quebec
April 18-20, 1990

Conference co-sponsored by the Canadian Nuclear Society and the American Nuclear Society

* *AECL CANDU*
** Nuclear Power Plants Authority, Cairo, Egypt

1990 April Avril 1990

AECL CANDU
2251 Speakman Drive
Mississauga Ontario
Canada L5K 1B2

EACL CANDU
2251, rue Speakman
Mississauga (Ontario)
Canada L5K 1B2

91XXXX

INFLUENCE OF GRAPHITE DISCS, CHAMFERS, AND PLENUMS ON TEMPERATURE DISTRIBUTIONS IN HIGH BURNUP FUEL

by

A. Ranger, M. Tayal, and P. Singh
AECL CANDU
Sheridan Park Research Community
Mississauga, Ontario L5K 1B2

and

I.A. El-Osery and K.A. Yasso
Nuclear Power Plants Authority
Cairo, Egypt

SUMMARY

Previous studies have demonstrated the desirability to increase the fuel burnups in CANDU reactors from 7–9 GW.d/t to 21 GW.d/t. At high burnups, one consideration in fuel integrity is fission gas pressure, which is predicted to reach about 13 MPa. The gas pressure can be kept below the coolant pressure (about 10 MPa) via a variety of options such as bigger chamfers, deeper dishes, central hole, and plenums. However, it is important to address the temperature perturbations produced by the bigger chamfers and plenums which in turn, affect the gas pressure.

Another consideration in fuel integrity is to reduce the likelihood of fuel failures via environmentally-assisted cracking. Insertion of graphite discs between neighbouring pellets will lower the pellet temperatures, hence, lower fission gas release and lower expansion of the pellet. Therefore, it is desired to quantify the effect of graphite discs on pellet temperatures.

Thermal analyses of different fuel element geometries: with and without chamfers, graphite discs, and plenums were performed. The results indicate that the two-dimensional distributions of temperatures due to the presence of chamfers, graphite discs, or plenums can have a significant impact on the integrity of high burnup fuel as we have been able to quantify in this paper.

EFFETS DES DISQUES EN GRAPHITE, DES CHANFREINS ET DES CHAMBRES D'EXPANSION SUR LA DISTRIBUTION DE LA TEMPÉRATURE DANS LE COMBUSTIBLE AUX FORTES COMBUSTIONS MASSIQUES

par

A. Ranger, M. Tayal, et P. Singh
EACL CANDU
Sheridan Park Research Community
Mississauga (Ontario) L5K 1B2

et

I.A. El-Osery et K.A. Yasso
Nuclear Power Plants Authority
Le Caire, Égypte

RÉSUMÉ

Des études ont démontré qu'il y a avantage à augmenter la combustion massique (de 7 – 9 GWj/t à 21 GWj/t) dans les réacteurs CANDU. Aux fortes combustions massiques, si l'on veut assurer l'intégrité du combustible, il faut tenir compte de la pression des gaz de fission qui, selon les calculs, atteint environ 13 MPa. On peut, par divers moyens, faire en sorte que la pression des gaz reste inférieure à la pression du caloporteur (environ 10 MPa). Ainsi, on peut avoir recours à des chanfreins plus larges, des cuvettes plus creuses, des cavités centrales ou des chambres d'expansion. Toutefois, l'utilisation de chanfreins plus larges et de chambres d'expansion occasionne des perturbations de température dont il faut tenir compte, car elles influent sur la pression des gaz.

Un autre point à prendre en considération concernant l'intégrité du combustible, c'est qu'il faut réduire la probabilité de défaillances du combustible causées par la fissuration provoquée par le milieu ambiant. Il est possible d'abaisser la température des pastilles en plaçant des disques en graphite entre les pastilles juxtaposées, ce qui a pour effet de réduire la libération des gaz de fission et la dilatation des pastilles. Il est donc souhaitable de quantifier les effets des disques en graphite sur la température des pastilles.

On a effectué des analyses thermiques d'éléments combustibles de différentes géométries avec et sans chanfreins, disques en graphite et chambres d'expansion. Les résultats indiquent que la distribution de température dans deux dimensions due à la présence de chanfreins, de disques en graphite et de chambres d'expansion peut avoir un effet considérable sur l'intégrité du combustible aux fortes combustions massiques, comme il a été possible de le quantifier dans la présente communication.

TABLE OF CONTENTS

LIST OF TABLES

LIST OF FIGURES

1. INTRODUCTION

Atomic Energy of Canada Limited has programs underway to maintain and improve the competitive position of CANDU reactors by improving resource utilization and by reducing unit energy costs. The use of slightly enriched uranium (SEU) in CANDU has been identified as offering substantial returns via reduced fuel cycle cost [1,2].

SEU fuel increases the reactivity. The resulting increase in discharge burnup for SEU over natural uranium (NU) exceeds the increase in uranium feed requirements [1,2]. There is also a corresponding decrease in the volume of spent fuel.

The designers of CANDU 6 Extended Burnup Core (EBC) have identified the desirability to increase the core–average exit burnup to 21 GW.d/tU by the use of SEU. In comparison, the current CANDU reactors use natural uranium and have core–average discharge burnups of 7–9 GW.d/tU.

At extended burnups, one consideration is the integrity of CANDU fuel. One factor affecting the fuel integrity is fission gas pressure, which is predicted to reach about 13 MPa at high burnups. During normal operation, the fission gas pressure is designed to stay below the coolant pressure (about 10 MPa), keeping the sheath in contact and with the fuel. The gas pressure can be reduced via a number of options such as bigger chamfers, deeper dishes, central hole, and plenums. Using the fuel performance code, ELESTRES [3], the effects of bigger chamfers on gas pressure have been evaluated. But experiments show that bigger chamfers also reduce the total length over which the pellet contacts the sheath. This perturbs the two–dimensional distribution of temperatures in the pellet and increases the temperatures in the pellet, causing further gas release. Therefore, it is desired to calculate the two–dimensional temperature distribution in the pellet and to assess its impact on gas release. From this, the acceptable chamfer size can be determined.

Plenums provide another way of reducing the gas pressure by providing empty space within the fuel element to store the fission gas. In the presence of a plenum at the end of the pellet stack, estimate of temperature distributions in the fuel pellet, sheath endcap and endcap weld region is needed for assessment of stresses; plenum temperatures also influence the gas pressure.

Another factor affecting the fuel integrity at high burnups is environmentally–assisted cracking (EAC) of the sheath. It occurs when the irradiation–embrittled sheath experiences high tensile stresses, generally due to pellet expansion, in the presence of a corrosive internal environment provided by fission products. EAC can be alleviated by a variety of modifications to the design of the fuel elements. For example, insertion of graphite discs between adjacent pellets reduces pellet temperatures by providing a more efficient path for removal of heat from the centre of pellet, hence, lower fission gas release and lower expansion of the pellet.

As part of the overall analysis of the fuel integrity at extended burnups, the influence of chamfers, plenums, and graphite discs on pellet temperatures which in turn affect the gas release, were examined.

This paper first describes the methods and the computer code used to perform the thermal analysis. Then, the fuel element geometries and models are given, followed by a discussion of the results. Figure 1 illustrates the terms used in this paper.

2. METHODOLOGY

2.1 APPROACH

Thermal analyses of the fuel element and fuel element end with no graphite disc, no plenum, and pellets containing no chamfer were first performed to provide reference results to compare with. Then the chamfer model was studied. The temperature calculations included the pellet with different chamfer sizes and the sheath. The temperature calculations for the plenum end included the end pellet in the stack, the graphite disc, the plenum, the endcap, weld and the sheath. Based on an earlier study [4], fuel elements containing annular UO_2 pellets with graphite discs were finally simulated. The temperature calculations for the graphite disc model included the annular pellet, the sheath, and the disc.

The calculations considered axisymmetric conditions. That is, the rate of heat generation varied radially and axially along the pellet, but not around the circumference. Similarly, the geometry of the system and the boundary conditions (temperatures) were considered axisymmetric.

The analyses used finite element techniques which permitted accurate representations of the curved and inclined surfaces in the analyzed geometries. An in–house heat transfer computer code, FEAT [5] was employed for the analyses. For maximum accuracy [6], triangular finite elements arranged in hexagonal patterns were used for all models. The finite element meshes were coded via a digitizer.

2.2 THE FEAT CODE

FEAT is a general purpose finite element code for thermal analyses. It was used here to calculate the multidimensional temperatures in fuel elements that contain large chamfers in the pellets, in graphite–disc fuel, and also in fuel element ends which contain plenums.

The code can model: conduction; internal generation of heat; prescribed convection to a heat sink; prescribed temperatures at boundaries; prescribed heat fluxes on surfaces; and temperature–dependence of materials properties like thermal conductivity. Gaps between neighbouring surfaces (i.e. between the pellet and the sheath) can also be simulated through the 'gap' elements. The finite element method is used to solve the classical multidimensional equation for conduction of heat. Iterations are used for the non–linear part of the solution; this makes the code inexpensive to run. The predictions of the code compare well (within $\pm$5%) against independent analytical solutions and against thermocouple measurements in pressure tubes. The code predictions are also consistent with isotherms inferred from grain–growths and from voids in fuel pellets.

Previous studies have shown that ten or more nodes across the pellet radius provide a converged solution for pellet temperatures [5]. This scheme was followed in our simulations.

3. GEOMETRY AND MODEL

3.1 THE CHAMFER MODEL

The axisymmetric model of the fuel element is shown in Figure 2. The analyzed system was subdivided into a number of triangular finite elements. These finite elements represent the UO_2 fuel pellet and the sheath. In this chamfer model, there are 236 nodes connecting 381 finite elements of which, 11 are gap elements and 10 are surface elements.

We expect that most of the heat flows from the pellet to the sheath and then to the coolant because of the large temperature difference between the coolant and the fuel pellet. We expect very little or no heat flow from one pellet to another since adjacent pellets are at similar temperatures. For these reasons, adiabatic boundary condition was assumed at the pellet end.

Heat transfer between two contacting solids, e.g. between the pellet and the sheath, is modelled through the 'gap' elements. These gap elements are given associated surface areas and surface heat transfer coefficient values. Heat is transferred to the outside coolant via forced convection at surface elements on the outside of the sheath. The heat transfer coefficients: pellet/sheath (9 kW/m^2K) and sheath/coolant (50 kW/m^2K) are provided by the fuel performance code, ELESTRES. The effect of CANLUB which provides some protection to the sheath against the fission products, is included in the pellet/sheath heat transfer coefficient calculated by ELESTRES. The different chamfer axial lengths are simulated by assigning a very low heat transfer coefficient, 0.05 kW/m^2K, between the sheath and the chamfered part of the pellet. The thermal conductivities of the UO_2 pellet and of the Zircaloy cladding are given in MATPRO [7] and are part of the FEAT code. They vary with temperature. The radial distribution of heat generation rate within the pellet is again provided by the ELESTRES code. The pellet density is 10.6 g/cm^3.

Using the above model, thirteen FEAT cases were run to calculate the influence of chamfer on volume–average temperature distribution in the pellet. The first six cases covered the chamfer size (axial length) from 0.0 to 2.08 mm at a linear power of 55 kW/m and a burnup of 200 MW.h/kgU. The other seven cases simulated a chamfer size (axial length) of 0.65 mm with power ranging from 10 to 70 kW/m and at a burnup of 200 MW.h/kgU.

3.2 THE PLENUM MODEL

Axisymmetric models of the fuel element ends without and with the plenum are shown in Figures 3a and 3b, respectively. The finite elements represent the UO_2 fuel pellet, Zircaloy endcap and sheath, and the filling and fission gases that are contained within the fuel element. For geometry 1 (without the plenum), 561 nodes, 909 triangular elements and 31 surface elements were used. For geometry 2 (with the plenum), 786 nodes, 1100 triangular elements and 47 surface elements were used.

Previous study [5] has indicated that there is very little axial heat conduction from the first pellet to the second pellet at the fuel element end. Therefore, only one pellet was included in the mesh. The filling gas and the released fission gases are modelled as conducting finite elements. A negligible heat flow via convection is expected and therefore ignored. For the purposes of calculating thermal conductivity of the gas within the fuel element, the released fission gas was assumed to consist of xenon and krypton. These elements form the overwhelming proportion of the released gases. Most of the heat flow is through the solid contact at endcap/plenum or endcap/pellet compared to very small flow through the gas in the gap.

As stated in the previous section, the thermal conductivities of UO_2 pellet and Zircaloy cladding are as per MATPRO [7] and are part of the FEAT code. The radial distribution of heat generation rate within the pellet is provided by the ELESTRES code. Heat transfer between two contacting solids is modelled through the 'gap' elements. Based on the ELESTRES results and previous study [4], there remains some uncertainty in the heat transfer coefficients: fuel to sheath, fuel to disc, disc to plenum, plenum to endcap, fuel to endcap, disc to sheath, and plenum to sheath. Therefore, a sensitivity study of temperatures to heat transfer coefficients was performed on the two geometries (i.e. with and without plenum). Table 1 lists the various cases along with the values of the parameters. The base cases are marked. The thermal conductivities of graphite used are: 120 W/m.K at 20°C; 65 W/m.K at 500°C; and 40 W/m.K at 1000°C. Linear interpolation is used in between.

3.3 GRAPHITE DISC MODEL

Figure 4 shows the axisymmetric model of the fuel element with graphite disc. Based on an earlier study [4], annular fuel pellet was chosen for the graphite disc model. The finite elements represent the UO_2 fuel pellet, the central hole, the graphite disc, the graphite disc hole, and the sheath. In this model, 328 nodes connecting 501 finite elements were used. Of the 501 finite elements, there were 13 surface elements and 31 gap elements.

The heat transfers between the pellet/sheath, pellet/disc, and disc/sheath are modelled though the 'gap' elements. The heat transfer coefficients: pellet/sheath (9 kW/m^2K) and sheath/coolant (50 kW/m^2K), are provided by the ELESTRES code. Based on the previous experimental measurement of corrosion rates in superheated steam, the heat transfer coefficients for pellet/disc and disc/sheath used are 3.21 kW/m^2K and 9.64 kW/m^2K, respectively. The thermal conductivities of graphite are as given in Section 3.2.

Eighteen FEAT cases were performed to examine the influence of graphite discs on volume–average and centreline temperatures. The first eight cases were simulated in the absence of graphite discs with linear power ranging from 10 to 70 kW/m and at a burnup of about 200 MW.h/kgU. In these cases, very small heat transfer coefficients were assigned between the pellet and the disc and between the disc and the sheath to simulate the absence of graphite discs. The other 10 cases were simulated with graphite discs. The linear power ranged from 10 to 80 kW/m at a burnup of 200 MW.h/kgU.

4. RESULTS AND DISCUSSION

4.1 EFFECT OF CHAMFER ON PELLET TEMPERATURES

The results for the thirteen cases as described in Section 3.1 are plotted in Figures 5a and 5b. Both figures show the increase in pellet volume–average temperature as a result of increasing either the chamfer size or power. From Figure 5a, the increase in pellet volume–average temperature is about 121 K due to the increase of chamfer axial length from the nominal design of 0.2 mm to 0.75 mm, at a power of 55 kW/m. This can be translated into an equivalent increase in power of about 5.4 kW/m, from 55 to 60.4 kW/m as shown in Figure 5b. This temperature effect predicted by FEAT was then used in ELESTRES as a scaling factor in the gas pressure calculation.

Figure 6 shows the pellet midplane temperatures (i.e. at surface and centreline) and maximum temperatures at pellet surface and pellet centreline as a function of chamfer axial length at a power of 55 kW/m and at a burnup of 200 MW.h/kgU. It can be seen that the perturbation (sharp gradient) is the highest for the maximum temperature at pellet surface around the chamfer region. Figure 7 gives the temperature distributions along the pellet length at three different radial locations: at the pellet surface, at a radial depth of about 0.7 mm, and at the pellet centreline. In this case, the power is at 55 kW/m and the pellet has a chamfer with an axial length of 0.75 mm. Again, it can be seen that the temperature perturbation is the highest around the chamfer region at the pellet surface. The temperature profile at the pellet centreline is not influenced by the chamfer and is essentially flat.

4.2 EFFECT OF PLENUM ON TEMPERATURE DISTRIBUTIONS

A parametric analysis was done on two geometries, i.e. with and without the plenum. Maximum temperatures attained within each component/region are summarized in Table 2. In the absence of a plenum, the maximum temperature is 2107°C at the pellet centre, 292°C in the weld region and 481°C in the endcap. In the presence of a plenum, the maximum temperature at the pellet centre is 2050°C, 260°C in the weld region and 281°C in the endcap. There is hardly any heat flow to the endcap and the weld region when the plenum is present. The maximum temperatures in the plenum and disc are 421°C and 533°C respectively.

The analysis results are also summarized via isotherms (temperature contours) in different components as given in Figures 8 and 9 for base cases 1 (no plenum) and 5 (with plenum), respectively. Figure 8 shows that the temperature difference, axially across the endcap thickness near the element centreline, is about 100°C. The location of the pellet/endcap contact depends on, among others, the details of the element design and on the operating conditions. For the particular conditions studied in this analysis, the contact occurred away from the axial centreline. The temperature in the endcap is about 40–100°C higher at the point of pellet/endcap contact than at the centreline of the endcap.

When comparing the isotherms in the plenum end (Figure 9) with the ones from the element end without plenum (Figure 8), it can be seen that the pellet centreline temperature is slightly lower because plenum provides a high–conduction path to the coolant. The endcap weld region is cooler which is important in the assessment of stresses. For example, the cooler endcap weld region would raise its yield strength. Hence, the plastic strains would be slightly lower. Hydriding and delayed hydride cracking (DHC) will exist at these lower temperatures, however, no major problem is seen due to the lower stress levels.

In general, without the plenum, the endcap temperature varies a great deal with the change in heat transfer coefficient between the pellet and the endcap. The maximum temperatures (see Table 2) vary from about 310°C for a low value of heat transfer coefficient to about 480°C for a high value of heat transfer coefficient. Other areas are hardly affected.

In the presence of plenum, the effect of different heat transfer coefficients on endcap, weld region and sheath temperatures is very small. Plenum and disc are the only components affected.

4.3 EFFECT OF GRAPHITE DISC ON PELLET TEMPERATURES

Eighteen FEAT cases were run to calculate the influence of graphite discs on volume–average and centreline temperatures. The results of volume–average temperatures and centreline temperatures with and without the discs at different power levels are plotted in Figures 10a and 10b. It should be noted that the figures show element ratings not pellet ratings. That is, the calculations assumed that for a given element rating, the pellets in the graphite–disc fuel operate at a higher volumetric–heat–generation rate to compensate for the heat not produced in the graphite.

From Figure 10a, the graphite–disc fuel at 40 kW/m has the same peak temperature in the pellet at the endplane as normal fuel at 55 kW/m, giving an 'advantage' of 15 kW/m in favour of graphite–disc fuel. This gain in power was fed back to ELESTRES as a scaling factor to determine the influence of graphite discs on ridge strain. Similarly, for the volume–average temperature (see Figure 10b), the corresponding advantage is about 6.4 kW/m.

5. CONCLUSIONS

Bigger chamfers increase the temperatures in the pellet. The temperature perturbation is manifest around the chamfer region of the pellet.

In the presence of a plenum, the temperatures at the endcap and weld region are lower. They are insensitive to values of heat transfer coefficients in the path of heat flow from the pellet to the endcap. They are essentially governed by the coolant temperature. They give higher zircaloy yield strength and this would result in slightly smaller plastic strains in comparison with those from the 'no plenum' geometry (with other conditions equal).

The reduction in pellet temperature due to the presence of graphite discs points to the significant benefits of graphite–disc fuel in areas of gas release and of ridge strains.

In conclusion, the two–dimensional distributions of temperatures due to the presence of chamfer, graphite disc, or plenum can have a significant impact on the integrity of high burnup fuel as we have been able to quantify in this paper.

ACKNOWLEDGEMENT

The authors would like to thank R. Sejnoha and M. Gacesa for their comments and support during the preparation of this paper.

REFERENCES

1. A.D. Lane, F.N. McDonnell, "Incentives for Slightly Enriched Uranium in CANDU", International Conference on CANDU Fuel, Canadian Nuclear Society, Chalk River, 1986 October 6–8, p. 624–630.
2. J.R. Hardman, A.C. Mao, A.R. Dastur, "The Use of Advanced Fuel Cycles in CANDU Plant Optimization", Tenth Annual Conference, Canadian Nuclear Society, Ottawa, Canada, 1989.
3. M. Tayal, "Modelling CANDU Fuel Under Normal Operating Conditions: ELESTRES Code Description", AECL–9331, February 1987.
4. R.D. MacDonald, I.J. Hastings, "Graphite Disk UO_2 Fuel Elements Designed for Extended Burnups at High Powers", Nuclear Technology, Volume 71, November 1985, p. 430–444.
5. M. Tayal, "The Finite Element Code FEAT to Calculate Temperatures in Solids of Arbitrary Shapes", Nuclear Engineering and Design, 114 (1989), p. 99–114.
6. T. Udoguchi, H. Okamura, T. Kano, Y. Nozue, "An Error Analysis of Various Finite Element Patterns", Bulletin of the Japanese Society of Mechanical Engineers, 16, 102 (1973), p. 1803–1813.
7. P.R. MacDonald, L.B. Thompson, (edited and compiled), "MATPRO–Version 09: A Handbook of Materials Properties for Use in the Analysis of Light Water Reactor Fuel Rod Behaviour", Report TREE–NUREG–1005, EG & G Idaho, Inc., 1976.

TABLE 1: THERMAL ANALYSIS CASES FOR THE PLENUM MODEL

	Heat Transfer Coefficient (kW/m^2K)					
Case	Fuel to Sheath	Disc or Plenum to Sheath	Pellet to Endcap	Pellet to Disc	Disc to Plenum	Plenum to Endcap
No–Plenum						
1*	15.6	N.A.	10.0	N.A.	N.A.	N.A.
2	40.0	N.A.	10.0	N.A.	N.A.	N.A.
3	15.6	N.A.	$1.0x10^6$	N.A.	N.A.	N.A.
4	15.6	N.A.	0.1	N.A.	N.A.	N.A.
Plenum–End						
5*	15.6	15.6	N.A.	10.0	10.0	10.0
6	40.0	40.0	N.A.	10.0	10.0	10.0
7	15.6	1.0	N.A.	10.0	10.0	10.0
8	15.6	15.6	N.A.	$1.0x10^6$	$1.0x10^6$	$1.0x10^6$
9	15.6	1.0	N.A.	0.1	0.1	0.1

* Base Case

N.A. – not applicable

TABLE 2: MAXIMUM COMPONENT TEMPERATURES IN THE ABSENCE / PRESENCE OF A PLENUM

	Maximum Temperature in Component (^{0}C)					
Case No.	Endcap	Weld Region	Sheath	Pellet	Plenum	Disc
No–Plenum						
1*	437	290	320	2071	N.A.	N.A.
2	429	288	319	2006	N.A.	N.A.
3	481	292	319	2063	N.A.	N.A.
4	309	281	321	2107	N.A.	N.A.
Plenum–End						
5*	272	260	319	2040	361	387
6	270	260	320	1974	343	365
7	281	260	320	2044	418	447
8	276	260	320	2039	369	379
9	260	260	319	2049	293	531

* Base Case

N.A. – not applicable

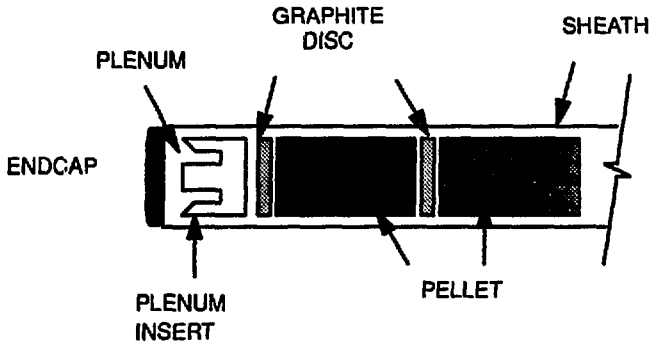

(a) FUEL ELEMENT

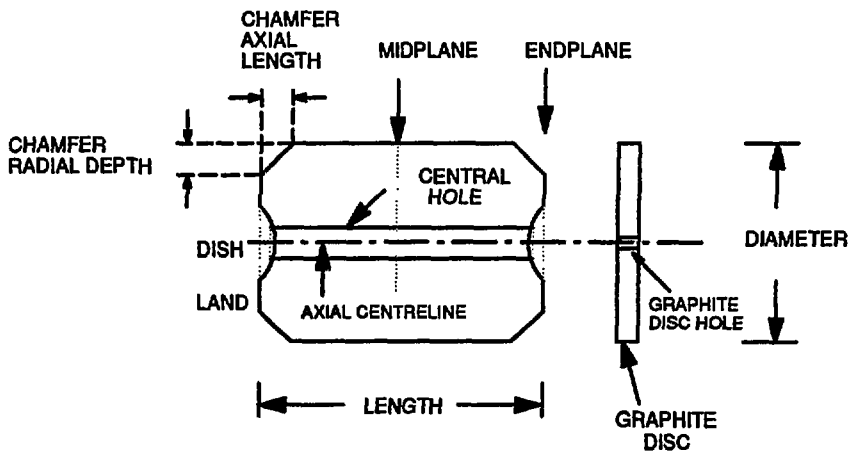

(b) PELLET AND GRAPHITE DISC

FIGURE 1: DEFINITIONS OF TERMS

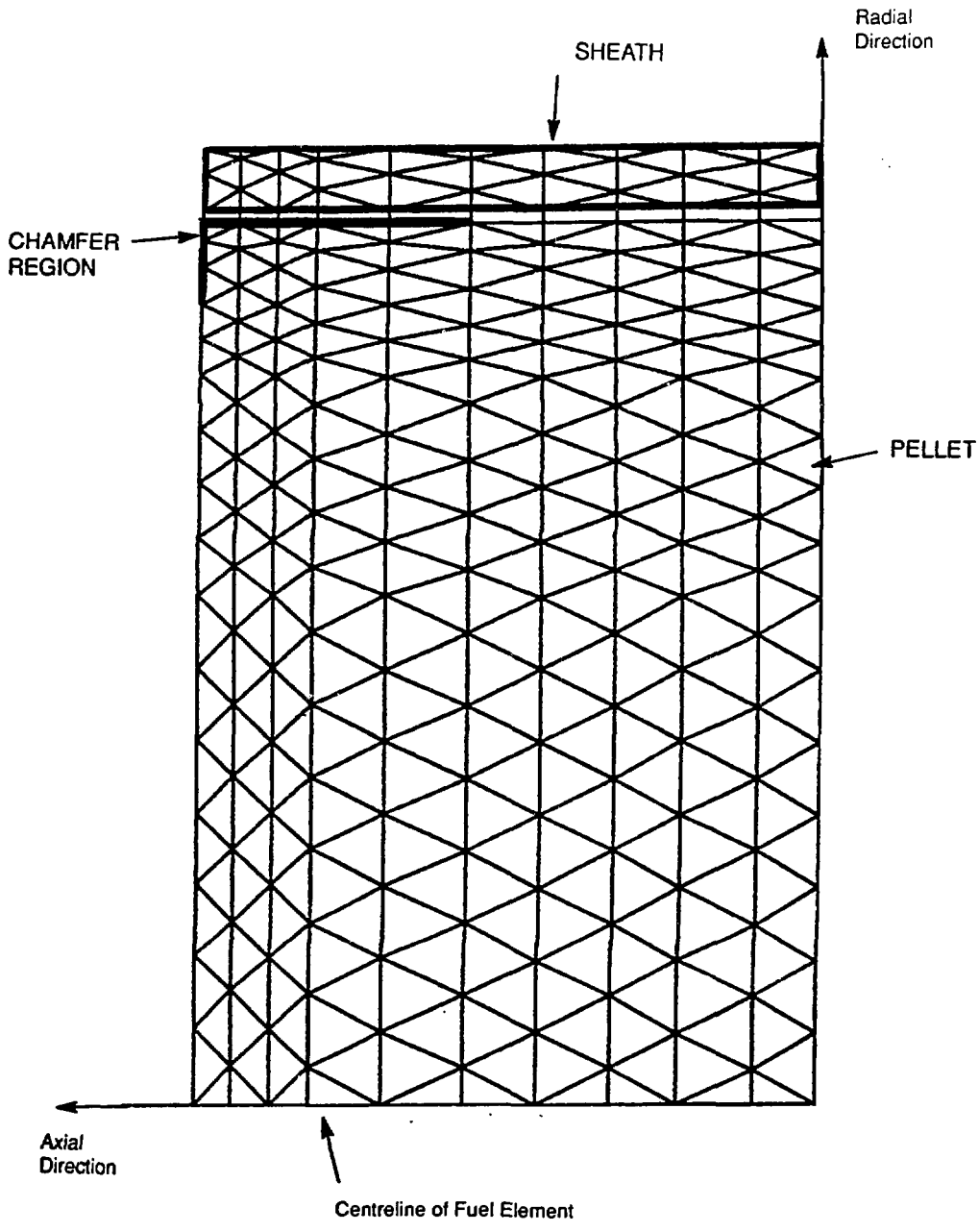

FIGURE 2: FINITE ELEMENT MESH FOR THE CHAMFER MODEL

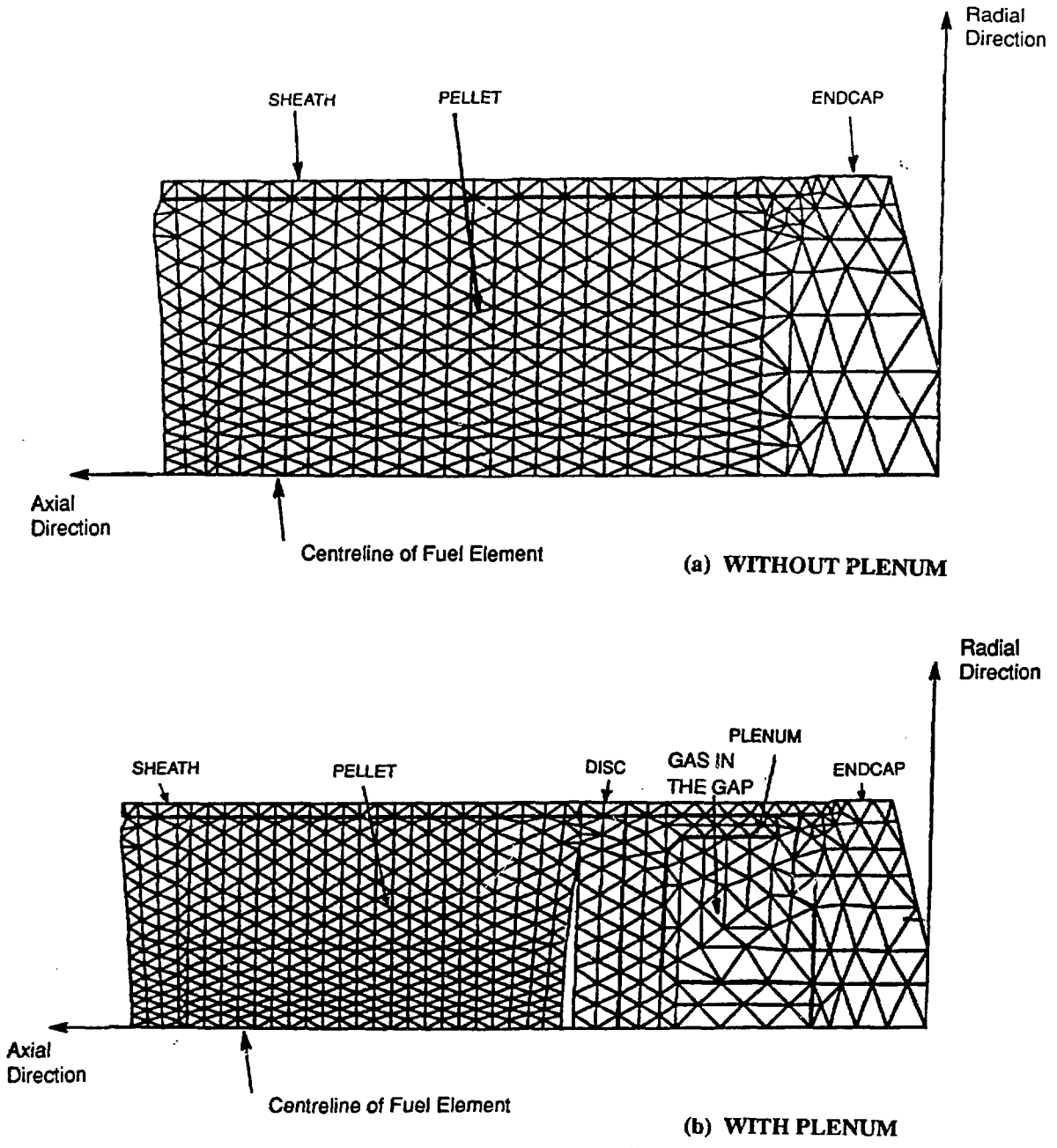

FIGURE 3: MODEL OF FUEL ELEMENT END

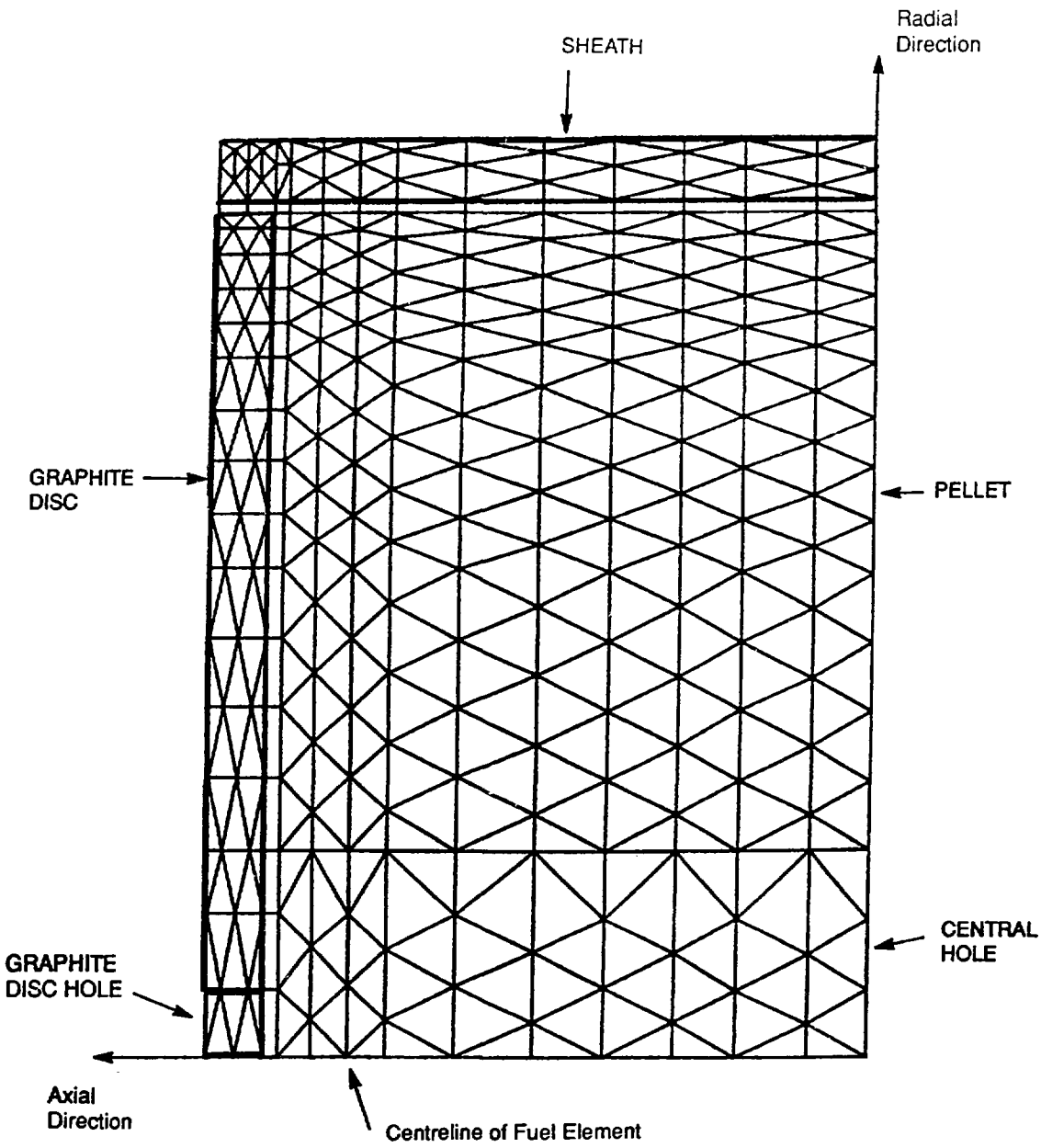

FIGURE 4: MODEL OF FUEL ELEMENT WITH GRAPHITE DISC

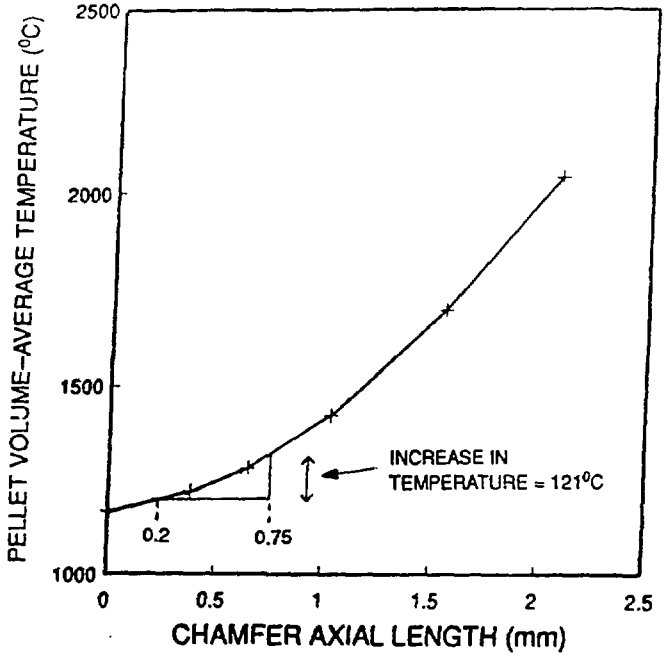

Figure 5 (a)

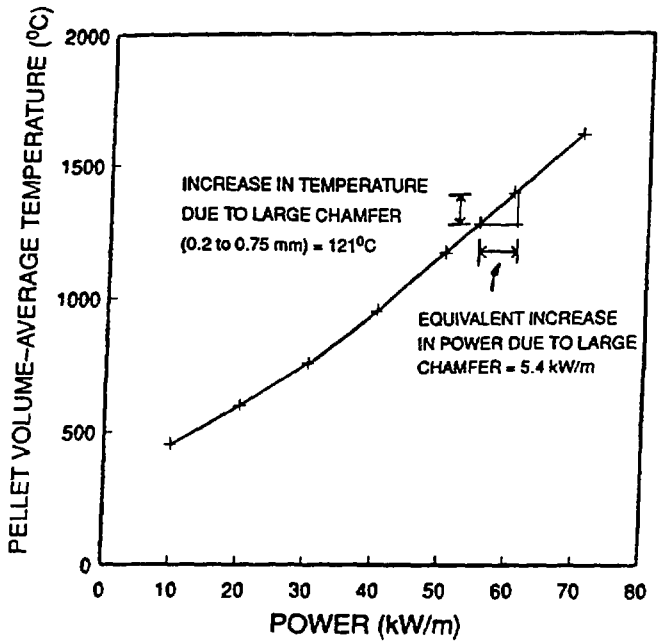

Figure 5 (b)

FIGURE 5: INFLUENCE OF CHAMFER ON PELLET TEMPERATURES

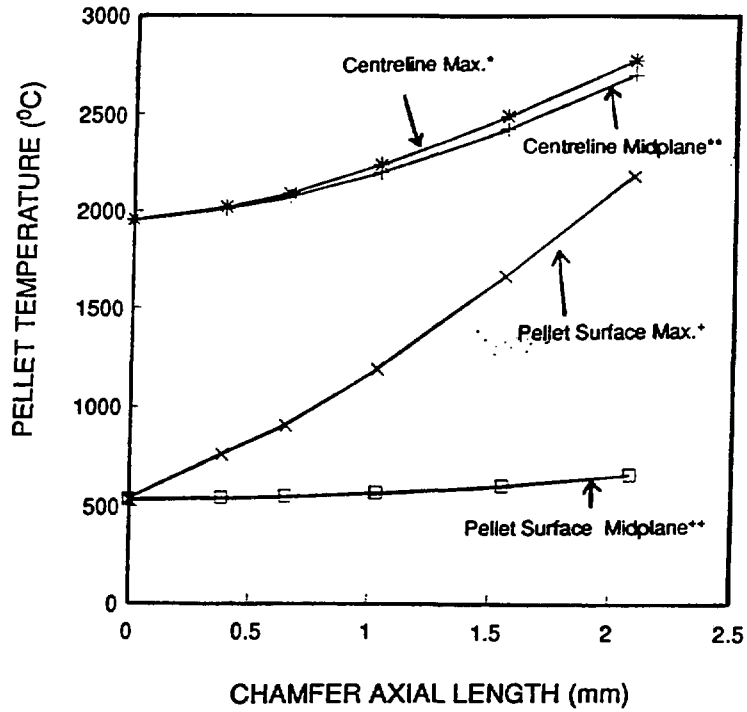

* means maximum temperature at the pellet centre at any axial location
** means pellet centreline temperature at the axial midplane
\+ means maximum temperature at the pellet surface at any axial location
\+\+ means pellet surface temperature at the axial midplane

FIGURE 6: EFFECT OF CHAMFER SIZE ON PELLET TEMPERATURES
(AT POWER = 55 kW/m)

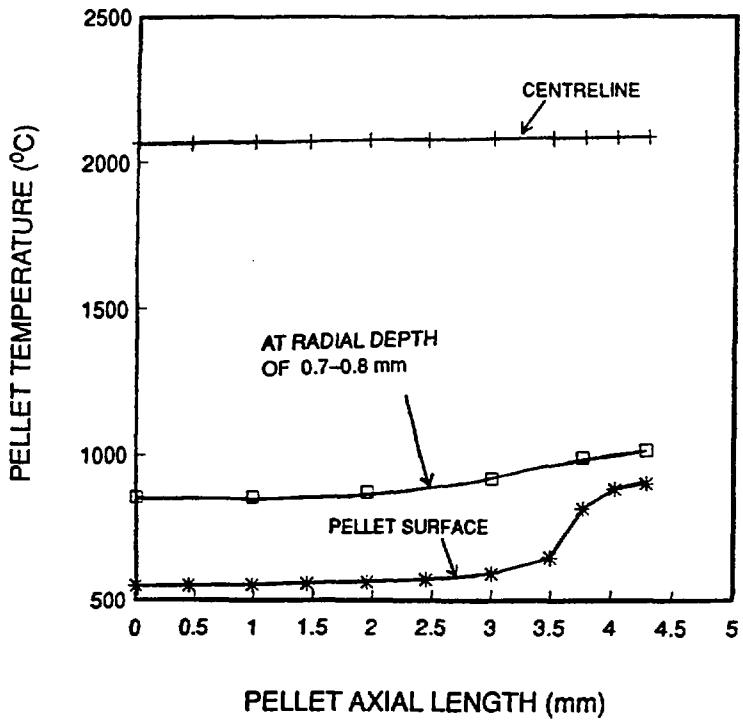

FIGURE 7: TEMPERATURE DISTRIBUTIONS IN A PELLET WITH 0.75 mm CHAMFER LENGTH (AT POWER = 55 kW/m)

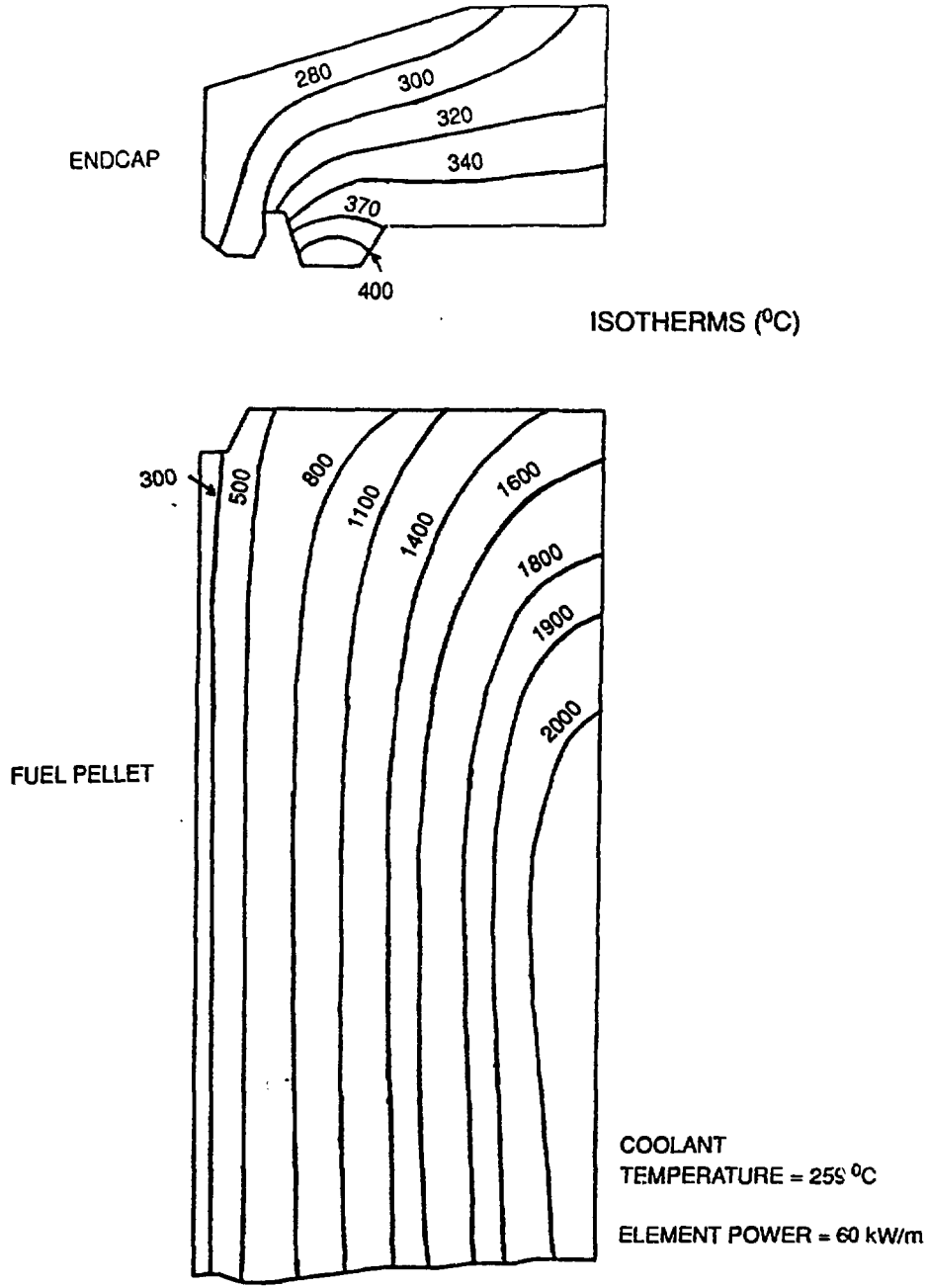

FIGURE 8: TEMPERATURE DISTRIBUTIONS AT PELLET END WITHOUT PLENUM

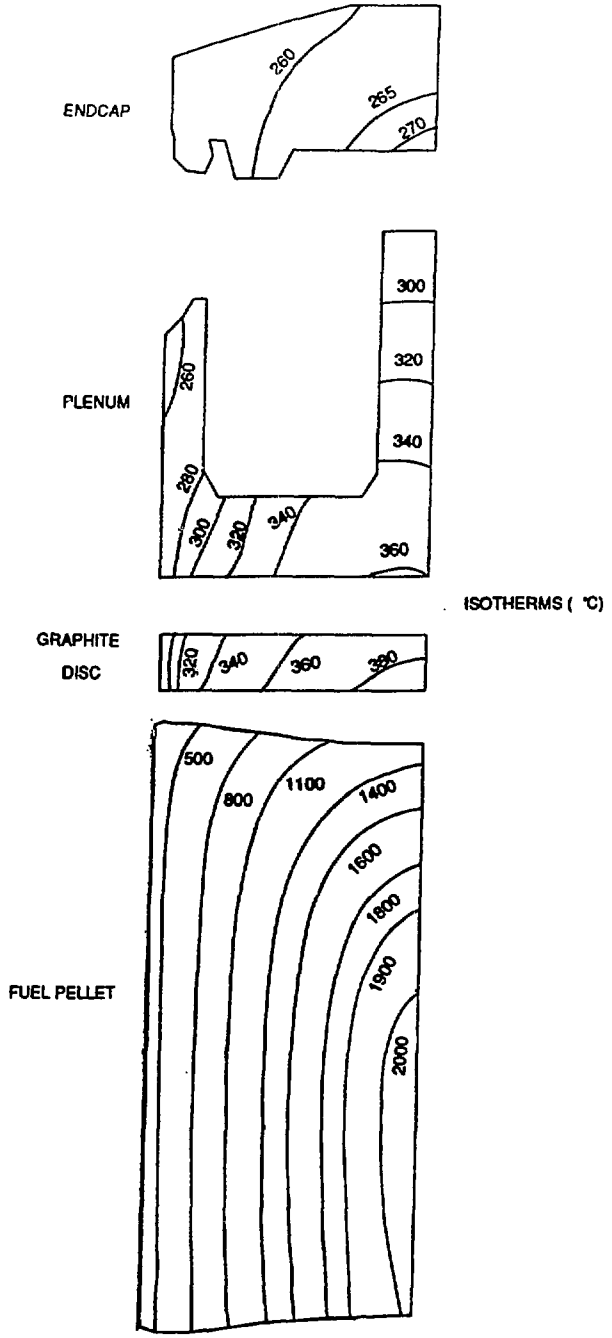

FIGURE 9: TEMPERATURE DISTRIBUTIONS AT PELLET END WITH PLENUM

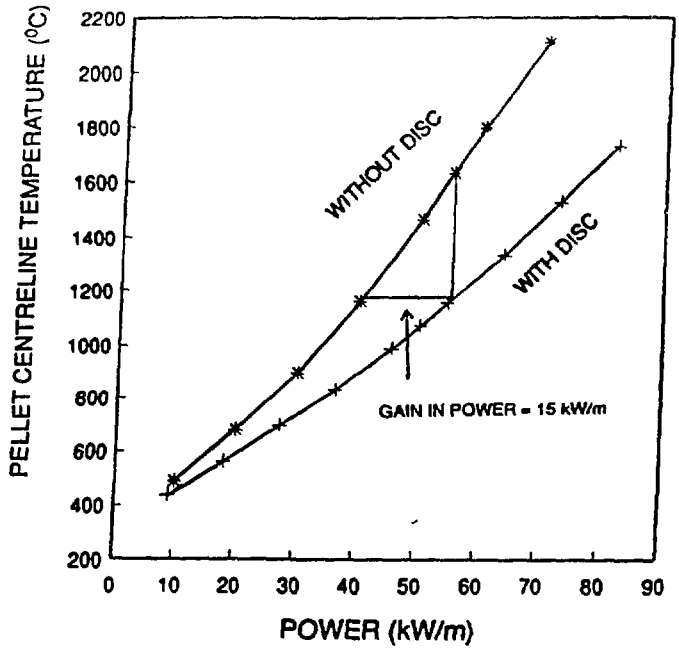

Figure 10 (a)

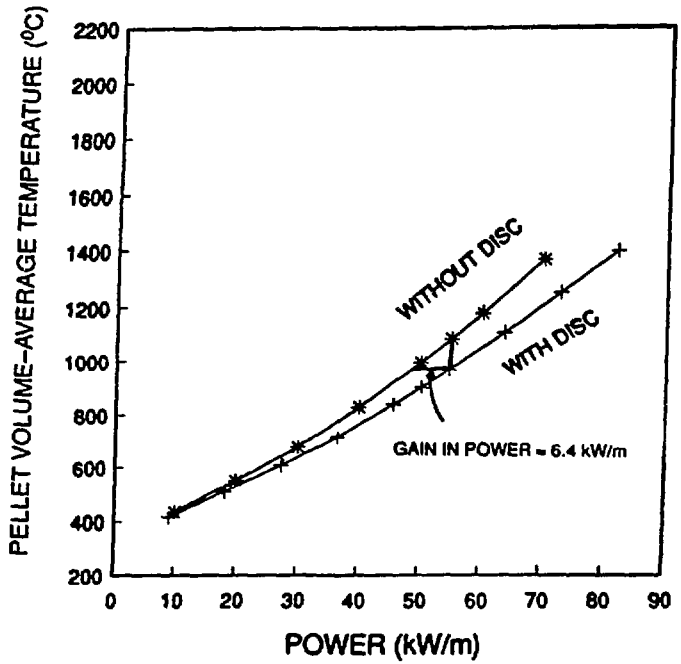

Figure 10 (b)

FIGURE 10: INFLUENCE OF GRAPHITE DISCS ON PELLET TEMPERATURES